Research note

Parkinson's pointers' potential perfidy! ★

Alan G. Jones *Lithospheric Geophysics, Geological Survey of Canada*
1 Observatory Crescent, Ottawa, Ontario K1A 0Y3, Canada

Summary. The geomagnetic induction community often employs arrows to display, in a qualitative fashion, the effects of electromagnetic induction in a given region. It is widely accepted that the reversed real induction arrow – or 'Parkinson' arrow – points *towards* current concentrations, which are interpreted as zones of high internal electrical conductivity. In this note, the frequency characteristics of an embedded inhomogeneity are studied in detail, and it is demonstrated that the above assertion may be false, i.e. that at sufficiently high frequencies these arrows may point *away* from zones of high internal conductivity. This effect is small, and is shown to be the case whenever the surface observation site is at a location such that it is sensing the return current flow associated with the anomalous horizontal electric field. The use of *anomalous transfer functions* is emphasized to aid in the qualitative assessment of induction in the region.

Key words: Induction arrows, conductivity anomalies, Geomagnetic Deep Sounding, Parkinson arrows, Wiese vectors

Introduction

Since its inception with Parkinson's original work on the subject (Parkinson 1962), the 'Parkinson arrow', and its closely related equivalent the 'Wiese vector' (Wiese 1962), has received widespread acceptance by the geomagnetic induction community. The 'Parkinson arrow' is defined as the horizontal projection of the downward normal to the 'Parkinson plane' – or 'preferred plane' – defined by Parkinson (1959), in which the variations of magnetic field preferentially occur.

The use of arrows to illustrate, in both a quantitative and qualitative manner, induction in an earth in which the electrical conductivity varies laterally increased significantly after Schmucker (1964, 1970), and independently Everett & Hyndman (1967) and Edwards, Law & White (1971), laid the foundation for a transfer function analysis of the interrelationship between the horizontal and vertical magnetic field components. In the complete treatment of Schmucker, the transfer functions $[z_x(\omega), z_y(\omega)]$ of the two-input/single output linear system are sought which relate the *anomalous* vertical magnetic field component $H_z^a(\omega)$ to

★ Geological Survey of Canada Publication 14286.

40*

the *normal* horizontal magnetic field components $[H_x^n(\omega), H_y^n(\omega)]$ at a given frequency ω,

$$H_z^a(\omega) = z_x(\omega) H_x^n(\omega) + z_y(\omega) H_y^n(\omega) + \epsilon \tag{1}$$

by reducing the error ϵ in some manner (usually least-squares). The necessity of undertaking a separation of the *total* field components into their constitutive *normal* and *anomalous* parts obviously places a severe restriction on the potential application of equation (1). Accordingly, the estimates of the transfer functions $[A(\omega), B(\omega)]$ of the linear system which defines a regression of the *total* horizontal magnetic field components $[H_x^t(\omega), H_y^t(\omega)]$ onto the *total* vertical magnetic field component $H_z^t(\omega)$, viz.,

$$H_z^t(\omega) = A(\omega) H_x^t(\omega) + B(\omega) H_y^t(\omega) + \epsilon \tag{2}$$

are most often determined and subsequently interpreted. The conditions under which $[A(\omega), B(\omega)]$ reasonably approximate $[z_x(\omega), z_y(\omega)]$ have been detailed by many workers (see e.g. Banks 1973; Alabi, Camfield & Gough 1975; Jones 1981a). However, provided that the source field is sufficiently uniform such that $H_z^t(\omega)$ contains an insignificant amount of *normal* vertical field $H_z^n(\omega)$, then it is obviously of little consequence in the modelling stage if the transfer functions defined by equation (1), or those defined by equation (2), are used. Indeed, if a separation into normal and anomalous parts is possible, Summers (1981, 1982) and Jones (1983, 1986) have argued for the adoption and use of *anomalous transfer functions* $[A_a(\omega), B_a(\omega)]$ which relate the *anomalous* vertical magnetic field component to the *anomalous* horizontal magnetic field components, viz.,

$$H_z^a(\omega) = A_a(\omega) H_x^a(\omega) + B_a(\omega) H_y^a(\omega) + \epsilon. \tag{3}$$

Having derived estimates of either $[z_x(\omega), z_y(\omega)]$ or $[A(\omega), B(\omega)]$, the majority of workers choose to display these by defining 'induction arrows', occasionally erroneously termed 'induction vectors' (see Parkinson 1983, p. 333). The 'in-phase' — or 'real' — arrow is defined by

$$\mathbf{c}^R(\omega) = -z_x^R(\omega)\mathbf{i} - z_y^R(\omega)\mathbf{j} \tag{4a}$$

and the 'quadrature' — or 'imaginary' — arrow by

$$\mathbf{c}^I(\omega) = +z_x^I(\omega)\mathbf{i} + z_y^I(\omega)\mathbf{j} \tag{4b}$$

(Schmucker 1970, p. 23), where $\mathbf{i}, \mathbf{j}$ are the Cartesian unit vectors towards magnetic north and east, and superscripts 'R' and 'I' refer to real and imaginary parts, respectively. Note that $\mathbf{c}^R$ is chosen to have a negative orientation to be in accordance with the orientation of the Parkinson arrow.

The relationships between the various arrows and graphical plots detailing the interrelationship between the relevant magnetic field components have been reviewed by Gregori & Lanzerotti (1980). However, the reader should be aware of the implicit assumptions made by these authors when they express relationships between the real 'Schmucker' arrow (defined by equation 4a) and the Parkinson and Wiese arrows (see the discussions on this review paper by Jones 1981b and Wolf 1982).

According to conventional wisdom, the Parkinson arrow and the real Schmucker arrow point 'towards zones of high, and away from zones of low, internal conductivity' (Schmucker 1970, p. 23). This supposed truism is to be found in many papers dealing with geomagnetic depth sounding (GDS) data, e.g. Gough, McElhinny & Lilley (1974, p. 354); Woods & Lilley (1979, p. 452); Greenhouse & Bailey (1981, p. 1271); Rokityansky (1982 p. 286); Wolf (1982, p. 520); Gough & Ingham (1983 p. 816); Prugger & Woods (1984 p. 7777). Other workers in the field have preferred to state that the real arrows, when

reversed, point towards internal current concentrations, e.g. Edwards *et al.* (1971, p. 309); Hyndman & Cochrane (1971 p. 434); Banks (1973 p. 344); Bailey *et al.* (1974 p. 130); Hutton & Jones (1980 p. SI 144); Camfield (1981 p. 560); Jones (1981a p. 30); Kurtz (1982 p. 377); Ingham, Bingham & Gough (1983 p. 603); Mareschal, Musser & Bailey (1983 p. 1437); Handa & Camfield (1984 p. 536); Gupta *et al.* (1985 p. 38).

It is the purpose of this note to discuss the frequency-dependence of an isolated anomaly, and to illustrate that the above assertions may, under certain circumstances, be false, i.e. that the Parkinson arrow and the real Schmucker arrow point *away* from the zone of high internal electrical conductivity, and *away* from the location of current concentration.

Model

The model employed to illustrate the previous, perhaps startling, statement is shown in Fig. 1 and was studied earlier by Summers (1981). However, this author was unable to reproduce Summers' results (his figs 3a, b), and we note that Wolf (1983) has already questioned the correctness of Summers' numerical code. The top of the prism, of resistivity 10 Ωm, is 60 km from the Earth's surface, within a host medium of 200 Ωm. Accordingly, at a period of 72 s the top of the prism is one skin depth below the surface, where the skin depth δ of an electromagnetic (EM) field is given by $\delta = \sqrt{2/\omega\mu\sigma}$, ω being the radian frequency of interest, μ and σ the permeability and electrical conductivity respectively of the medium. At this depth, the EM field has an amplitude of $1/e$ of its surface value, and a phase which lags the surface field by one radian. However, these amplitude and phase ratios are only meaningful in the *absence* of the conducting prism — the very existence of the inhomogeneity makes meaningless any discussion of the amplitude and phase characteristics of the magnetic and electric fields at a given depth from skin depth type arguments. If the conductivity of the
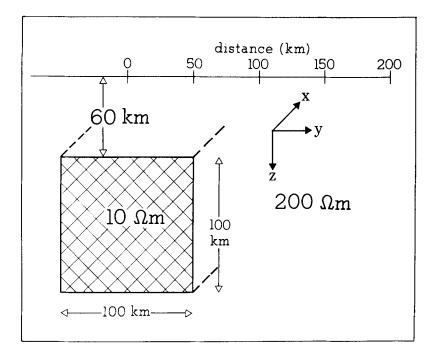

Figure 1. The geometry and parameters of the model studied and coordinate system used.

prism were infinite, then there could not be any penetration of the electric field into the block, and obviously the electric field would have zero amplitude on all block boundaries. If the 10 Ωm block were not bounded in the y-direction, i.e., a layered 1-D model, then the electric field amplitude and phase (normalized to the surface field) on the block's upper surface for a 72 s EM wave would be 0.13° and −61° respectively, compared to 0.37 and −57.25° from skin depth attenuation in a uniform half-space.

Following Summers' suggestion (1981), it is instructive to consider the anomalous fields caused by the presence of the inhomogeneity. In Fig. 2 contours of $E_x^a(t)$ are illustrated, the instantaneous anomalous horizontal electric field along strike (E_x is the only electric field component that exists), in units of nV km^{-1} for a *normal* horizontal magnetic field of 1 γ in the *E-polarization* mode of induction at periods of 100 s (Fig. 2a) and 1000 s (Fig. 2b) at a time $-\pi/4$ radians. In a uniform half-space, the electric field leads the magnetic field by $\pi/4$, and in fact the electric field on the surface at $y = 0$ is within 6° of this value at both periods. Hence, this 'snapshot' gives a visual impression of the field pattern that is responsible for the in-phase anomalous magnetic fields. As can be seen by comparing the two figures, a radically different anomalous field pattern results at the two periods. At both periods, the anomalous electric field, and, accordingly, anomalous current density from $\mathbf{J} = \sigma\mathbf{E}$, is centred at a depth of 70−80 km at location $y = 0$. The maximum anomalous field strengths, for a 1 γ normal horizontal magnetic field, are $\approx$670 nV km^{-1} and $\approx$490 nV km^{-1} at 100 s and 1000 s periodicity respectively, i.e., anomalous current densities of 67 nA m^{-2} and 49 nA m^{-1}. Note that the fields at this position are *negative* i.e. they are opposed in direction to the incident horizontal electric field and result in the *total* horizontal electric field being reduced.

However, there is a fundamental difference between the fields at these periods. The contour along which the anomalous electric field goes through zero is mostly *below the surface* at 100 s period, whereas it is above the surface for locations directly over, and 'close' to, the anomaly at 1000 s, where 'close' for this case means $|y| < 450$ km. Beyond this zero contour, the anomalous electric field is positive, i.e. it is in the same sense as the incident normal electric field, and these fields can be thought of as associated with the return currents of the anomalous electric field (the return currents of the normal field are at 'infinity'). The zero contour is *totally* below the surface at all periods shorter than 72 s. At 72 s, the period at which the top of the body is at exactly one skin depth below the surface, this contour grazes the surface at $y = 0$. At all longer periods, this contour intersects the surface at a lateral distance from the anomaly which increases with increasing period, and is 45 km and 450 km at 100 s and 1000 s, respectively.

The anomalous electric field at 1000 s (Fig. 2b) may be thought of as the 'conventional' view of EM induction in an isolated conducting inhomogeneity. The field induces an anomalous magnetic field which, at the surface above and 'close' to the anomaly, is additive to the normal horizontal magnetic field, as shown in Fig. 3 (curve labelled *b*). Thus, a Fourier amplitude map of this total horizontal magnetic field component will display a *maximum* directly above the anomaly. The transfer function between the vertical magnetic field component H_z (which is H_z^a as $H_z^n = 0$) and the *total* horizontal magnetic field component H_y^t is as illustrated in Fig. 4b. Note that the real part of this function is positive for $0 < y < 450$ km, so that when the real induction arrow is derived, using equation (4a), it will point *towards* the conducting inhomogeneity.

However, the situation at 100 s is dramatically different. The surface anomalous electric field is everywhere in the same sense as the incident field, apart from locations directly above the body, i.e. $|y| < 45$ km, and hence the surface anomalous horizontal magnetic field is subtractive from the normal horizontal magnetic field. This results in a total magnetic field which is less than the normal horizontal magnetic field (see Fig. 3, curve *a*). Thus, a Fourier
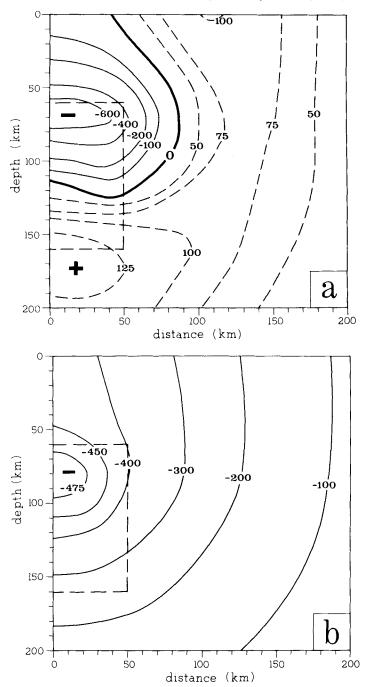
Figure 2. (a) Contours of the instantaneous anomalous horizontal electric field along strike, i.e. $E_x^a(t)$, in nV km^{-1} for an incident normal horizontal magnetic field of 1 γ with a periodicity of 100 s at a time of $-\pi/4$ radians (-12.5 s). The *full* lines are negative, i.e. they are opposed in direction to the incident field, whereas the *dashed* lines are positive. The zero contour is the location along which there is no instantaneous anomalous electric field. (b) As for (a) but for a period of 1000 s and at a time of -125 s. Note that the zero amplitude contour is not within this diagram, but does intersect the ground surface at ± 450 km.
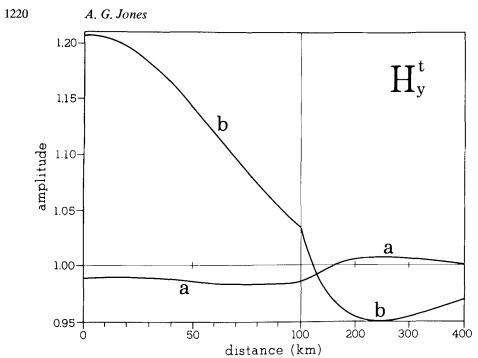
Figure 3. The amplitude of the total horizontal magnetic field component perpendicular to strike $|H_y^t(\omega)|$, for a normal incident magnetic field of 1 γ, at periods of 100 s (curve *a*) and 1000 s (curve *b*).
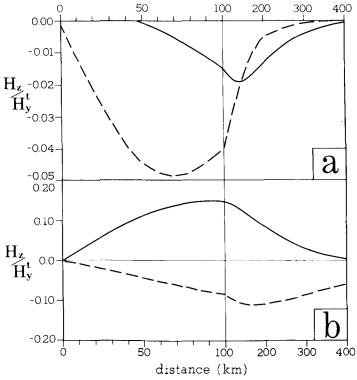

Figure 4. The ratio of the vertical field component to the total horizontal magnetic field component perpendicular to strike H_z/H_y^t at 100 s (a) and 1000 s (b). The *full* lines illustrate the real parts, whereas the *dashed* lines illustrate the imaginary parts. Note the difference in ordinate scales between (a) and (b).
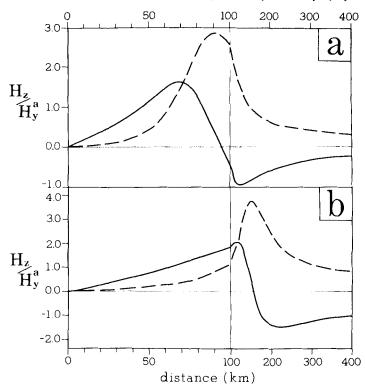
Figure 5. The ratio of the vertical field component to the anomalous horizontal magnetic field component perpendicular to strike H_z/H_y^a at 100 s (a) and 1000 s (b). The *full* lines illustrate the real parts, whereas the *dashed* lines illustrate the imaginary parts.

amplitude map of this component at this period will display a broad *minimum* above the anomaly, flanked by two *maxima* at some distance from it (in this case 250 km). Obviously, a Fourier map from a profile conducted between locations $y = 0{-}200$ km at this period would be erroneously interpreted as indicating a fault-like structure at $y \approx 150$ km. Also, the real induction vector defined by equation (4a) will be reversed and point *away* from the inhomogeneity (Fig. 4a). Note that directly above the structure, i.e. for $|y| < 45$ km, for this period Re (H_z/H_y^t) is virtually zero — it is, in fact, positive but exceedingly small (< 0.01). (Fig. 4a can be compared directly with fig. 3a of Summers (1981) — a major difference is obvious). It is also observed in the transfer function defined by equation (1), i.e. Re (H_z/H_y^n), and, in fact, this function is negative at all locations y. This effect is due to high frequency oscillations of the EM field and has long been exploited in controlled-source EM work. It manifests itself in the magnetotelluric technique as a high-frequency oscillation of the apparent resistivity curve. The effect is small, but it should be known and appreciated.

This apparent frequency-dependent inconsistency does not appear when the *anomalous* transfer functions, defined by equation (3), are used. In Fig. 5 are illustrated these functions, given by $H_z(\omega)/H_y^a(\omega)$, at 100s and 1000s period. (Fig. 5a can be compared directly with fig. 3b of Summers (1981), and large discrepancies are evident.) For $y > 0$, then Re (H_z/H_y^a) is always positive above the inhomogeneity, and out to some large value of y, and, hence, the reversed real anomalous induction arrows close to an inhomogeneity point towards it at all frequencies. Im (H_z/H_y^a) is positive for all $y > 0$, and, hence, reversed imaginary anomalous induction arrows *always* point towards an inhomogeneity at all

frequencies. However, as mentioned by Jones (1983), these arrows only indicate the location of *anomalous* zones in conductivity, they do not indicate if the anomalous zone is of higher or lower conductivity than the surrounding host rock.

Conclusions

The real induction arrow, or 'Parkinson arrow', does not always point *towards* a zone of higher conductivity or to current concentrations. At all frequencies higher than that at which the top of the body is one skin depth below the surface, the zero contour of the instantaneous anomalous horizontal electric field $E_x^a(\omega)$ is totally below the surface at a time of $-\pi/4$. Accordingly, the arrow, when reversed, will point *away* from the structure. The amplitudes of the transfer functions under these conditions are small — for the example considered herein, the maximum real and imaginary induction arrows at 100 s are −0.02 at $y = 140$ km and −0.05 at $y = 70$ km. However, given our increasing ability at obtaining high precision estimates of small-valued transfer functions (e.g. Jones & Jödicke 1984; Chave, Thomson & Ander 1985), due consideration must be given to the frequency-dependence of anomalies discussed herein. This is particularly important if the arrows, or the Fourier amplitude maps, are interpreted in a qualitative manner only. It is possible to perceive of a study that only derives GDS response information at periods shorter than that at which the anomaly is one skin depth below the surface, and in such a situation a totally erroneous qualitative interpretation might result. Accordingly, quantitative modelling of transfer function responses must be undertaken, and it must be ensured that the full frequency response of the anomaly is known.

Obviously, this situation of real arrows having an apparently erroneous orientation does not occur at any frequency whatsoever for anomalies that are exposed at the surface, for example the coast-effect.

Finally, it should be noted that Summers' calculations cannot be reproduced. This author derived all the calculations presented herein, including Figs 4(a, b), using two different modelling programmes, Madden's EMCDC (Madden 1973) and Ku's (Ku, Hsieh & Lim 1973), both of which are transmission surface analogues and have been checked against analytical solutions [d'Erceville & Kunetz's (1962) fault] by this author in their *B-polarization* implementations. With this problem in mind, perhaps authors' of new code should be requested to check their solutions against control models, for example the ones proposed by Zhdanov's COMMEMI project (Zhdanov & Varentsov, 1984), or the analytical *B-polarization* and *E-polarization* solutions for the model proposed by Weaver (Weaver, Le Quang & Fischer 1985, 1986), before publications describing the results of their code can be accepted.

Acknowledgments

References

Alabi, A. O., Camfield, P. A. & Gough, D. I., 1975. The North American Central Plains anomaly, *Geophys. J. R. astr. Soc.,* 43, 815–834. ·

Bailey, R. C., Edwards, R. N., Garland, G. D., Kurtz, R. & Pitcher, D. H., 1974. Electrical conductivity studies over a tectonically active area in eastern Canada, *J. Geomagn. Geoelectr.,* 26, 125–146.

Banks, R. J., 1973. Data processing and interpretation in Geomagnetic Deep Sounding, *Phys. Earth planet. Inter.,* 7, 339–348.

Camfield, P. A., 1981. Magnetometer array study in a tectonically active region of Quebec, Canada, *Geophys. J. R. astr. Soc.,* 65, 553–570.

Chave, A. D., Thomson, D. J. & Ander, M. E., 1985. On the robust estimation of power spectra, coherences, and transfer functions, *J. geophys. Res.,* submitted.

d'Erceville, E. J. & Kunetz, G., 1962. The effect of a fault on the earth's natural electromagnetic field, *Geophysics,* 27, 651–665.

Edwards, R. N., Law, L. K. & White, A., 1971. Geomagnetic variations in the British Isles and their relation to electrical currents in the ocean and shallow seas, *Phil. Trans. R. Soc.,* 270, 289–323.

Everett, J. E. & Hyndman, R. D., 1967. Geomagnetic variations and electrical conductivity structure in south-western Australia, *Phys. Earth planet. Inter.,* 1, 24–34.

Gough, D. I. & Ingham, M. R., 1983. Interpretation methods for magnetometer arrays, *Rev. Geophys. Space Phys.,* 21, 805–827.

Gough, D. I., McElhinny, M. W. & Lilley, F. E. M., 1974. A magnetometer array study in southern Australia, *Geophys. J. R. astr. Soc.,* 36, 345–362.

Greenhouse, J. P. & Bailey, R. C., 1981. A review of geomagnetic variation measurements in the eastern United States: implications for continental tectonics, *Can. J. Earth Sci.,* 18, 1268–1289.

Gregori, G. P. & Lanzerotti, L. J., 1980. Geomagnetic depth sounding by induction arrow representation: a review, *Rev. Geophys. Space Phys.,* 18, 203–209.

Gupta, J. C., Kurtz, R. D., Camfield, P. A. & Niblett, E. R., 1985. A geomagnetic induction anomaly from IMS data near Hudson Bay, and its relation to crustal electrical conductivity in central North America, *Geophys. J. R. astr. Soc.,* 81, 33–46.

Handa, S. & Camfield, P. A., 1982. Crustal electrical conductivity in north-central Saskatchewan: the North American Central Plains anomaly and its relation to a Proterozoic plate margin, *Can. J. Earth Sci.,* 21, 533–543.

Hutton, V. R. S. & Jones, A. G., 1980. Magnetovariational and magnetotelluric investigations in S. Scotland. In *Electromagnetic Induction in the Earth and Moon*, pp. 141–150, ed. Schmucker, U., AEPS-9, Centr. Acad. Publ. Japan, Tokyo and Reidel, Dordrecht, *Suppl. Iss. J. Geomagn. Geoelectr.*

Hyndman, R. D. & Cochrane, N. A., 1971. Electrical conductivity structure by geomagnetic induction at the continental margin of Atlantic Canada, *Geophys. J. R. astr. Soc.,* 25, 425–446.

Ingham, M. R., Bingham, D. K. & Gough, D. I., 1983. A magnetovariational study of a geothermal anomaly, *Geophys. J. R. astr. Soc.,* 72, 597–618.

Jones, A. G., 1981a. Geomagnetic induction studies in Scandinavia – II. Geomagnetic depth sounding, induction vectors and coast effect, *J. Geophys.,* 50, 23–36.

Jones, A. G., 1981b. Comment on 'Geomagnetic Depth Sounding by Induction Arrow Representation: A Review' by G. P. Gregori & L. J. Lanzerotti, *Rev. Geophys. Space Phys.,* 19, 687–688.

Jones, A.. G., 1983. The problem of 'current channelling': a critical review, *Geophys. Surv.,* 6, 79–122.

Jones, A. G., 1986. On the use of line current analogues in geomagnetic depth sounding, *J. Geophys.,* in press.

Jones, A. G. & Jödicke, H., 1984. Magnetotelluric transfer function estimation improvement by a coherence-based rejection technique. Contributed paper at '*1984 Annual SEG meeting*', held in Atlanta, Georgia, USA, 1984 December.

Ku, C. C., Hsieh, M. S. & Lim, S. H., 1973. The topographic effect in electromagnetic fields, *Can. J. Earth Sci.,* 10, 645–656.

Kurtz, R. D., 1982. Magnetotelluric interpretation of crustal and mantle structure in the Grenville Province, *Geophys. J. R. astr. Soc.,* 70, 373–397.

Madden, T. R., 1973. *Instruction Manual for EMCDC and EMUVC (EMCAL)*, Exploration Aids Inc., Needham, Mass.

Mareschal, J.-C., Musser, J. & Bailey, R. C., 1983. Geomagnetic variation studies in the southern Appalachians: preliminary results, *Can. J. Earth Sci.,* 20, 1434–1444.

Parkinson, W. D., 1959. Direction of rapid geomagnetic fluctuations, *Geophys. J. R. astr. Soc.,* 2, 1–14.

Parkinson, W. D., 1962. The influence of continents and oceans on geomagnetic variations, *Geophys. J. R. astr. Soc.,* 6, 441–449.

Parkinson, W. D., 1983. *Introduction to Geomagnetism*, Elsevier, New York.

Prugger, A. F. & Woods, D. V., 1984. The pattern of anomalous geomagnetic variation fields over the Midcontinent Gravity High, *J. geophys. Res.,* 89, 7773–7782.

Rokityansky, I. I., 1982. *Geoelectromagnetic Investigation of the Earth's Crust and Mantle*, Springer-Verlag, Berlin.

Schmucker, U., 1964. Anomalies of geomagnetic variations in the southwestern United States, *J. Geomagn. Geoelectr.*, **15**, 192–221.

Schmucker, U., 1970. Anomalies of geomagnetic variations in the southwestern United States, *Bull. Scripps Inst. Oceanogr.*, **13**, University of California Press.

Summers, D. M., 1981. Interpreting the magnetic fields associated with two-dimensional induction anomalies, *Geophys. J. R. astr. Soc.*, **65**, 535–552.

Summers, D. M., 1982. On the frequency response of induction anomalies, *Geophys. J. R. astr. Soc.*, **70**, 487–502.

Weaver, J. T., Le Quang, B. V. & Fischer, G., 1985. A comparison of analytical and numerical results for a two-dimensional control model in electromagnetic induction – I. B-polarization calculations, *Geophys. J. R. astr. Soc.*, **82**, 263–278.

Weaver, J. T., Le Quang, B. V. & Fischer, G., 1985. A comparison of analytical and numerical results for a two-dimensional control model in electromagnetic induction – II. E-polarization calculations, *Geophys. J. R. astr. Soc.*, in press.

Wiese, H., 1962. Geomagnetische Tiefentellurik, II, Die Streichrichtung der Untergrundstrukturen des elektrischen Widerstandes, erschlossen aus geomagnetischen Variationen, *Geofis. Pura Appl.*, **52**, 83–103.

Wolf, 1982. Comment on 'Geomagnetic Depth Sounding by Induction Arrow Representation: A Review' by G. P. Gregori & L. J. Lanzerotti, *Rev. Geophys. Space Phys.*, **20**, 519–521.

Wolf, D., 1983. Singular solutions to Maxwell's equations and their significance for geomagnetic induction, *Geophys. J. R. astr. Soc.*, **75**, 279–283.

Woods, D. V. & Lilley, F. E. M., 1979. Geomagnetic induction in central Australia, *J. Geomagn. Geoelectr.*, **31**, 449–458.

Zhdanov, M. S. & Varentsov, I. M., 1984. Progress report on the COMMEMI (Comparison of Modelling Methods in EM Induction) project. Contributed paper at '*Seventh Workshop on Electromagnetic Induction in the Earth and Moon*', held in Ile-Ife, Nigeria, 1984 August 15–22.